PHYSICAL REVIEW D **95,** 083007 (2017)

Propagation of cosmic rays in the AMS-02 era

Qiang Yuan (袁强),[1,2,*] Su-Jie Lin (林苏杰),[3] Kun Fang (方堃),[3] and Xiao-Jun Bi (毕效军)[3,†]

[1]*Key Laboratory of Dark Matter and Space Astronomy, Purple Mountain Observatory, Chinese Academy of Sciences, Nanjing 210008, People's Republic of China*

[2]*School of Astronomy and Space Science, University of Science and Technology of China, Hefei, Anhui 230026, People's Republic of China*

[3]*Key Laboratory of Particle Astrophysics, Institute of High Energy Physics, Chinese Academy of Science, Beijing 100049, People's Republic of China*

(Received 31 January 2017; published 19 April 2017)

In this work we use the newly reported boron-to-carbon ratio (B/C) from AMS-02 and the time-dependent proton fluxes from PAMELA and AMS-02 to constrain the source and propagation parameters of cosmic rays in the Milky Way. A linear correlation of the solar modulation parameter with solar activities is assumed to account for the time-varying cosmic ray fluxes. A comprehensive set of propagation models, with or without reacceleration or convection, has been discussed and compared. We find that only the models with reacceleration can self-consistently fit both the proton and B/C data. The rigidity dependence slope of the diffusion coefficient, δ, is found to be about 0.38–0.50 for the diffusion-reacceleration models. The plain diffusion and diffusion-convection models fit the data poorly. We compare different model predictions of the positron and antiproton fluxes with the data. We find that the diffusion-reacceleration models overproduce low energy positrons, while nonreacceleration models give better fit to the data. As for antiprotons, reacceleration models tend to underpredict low energy antiproton fluxes, unless a phenomenological modification of the velocity dependence of the diffusion coefficient is applied. Our results suggest that there could be important differences of the propagation for nuclei and leptons, in either the Milky Way or the solar heliosphere.

DOI: 10.1103/PhysRevD.95.083007

I. INTRODUCTION

The propagation of cosmic rays (CRs) in the Milky Way is a fundamental question to understand the origin and interactions of galactic CRs. It also provides us with a useful tool to probe the properties of the interstellar medium (ISM). It is well known that the charged CRs propagate diffusively in the galactic magnetic field, experiencing possibly the reacceleration, convection, spallation, and energy loss processes [1,2]. The propagation process can be described with the diffusive transport equation [1,3]. Depending on different simplifications, the transport equation can be solved analytically [4–8]. Also there were efforts to include most of the relevant processes and the observation-based astrophysical inputs, and to solve the propagation equation numerically, e.g., GALPROP [9,10] and DRAGON [11].

To understand the propagation of CRs is not only important for the CR physics itself, but also the basis of searching for the exotic signal from particle dark matter. The propagation of CRs couples closely with the production, leading to the entanglement between source parameters and propagation parameters. Fortunately, the spallation of the CR nuclei when colliding with the ISM produces secondary nuclei (with kinetic energy per nucleon unchanged). The ratio between those secondary nuclei and the parent nuclei cancels out the source information, leaving basically the propagation effect. Widely used are the boron-to-carbon (B/C) and subiron-to-iron [$(\mathrm{Sc}+\mathrm{Ti}+\mathrm{V})/\mathrm{Fe}$] ratios. The unstable-to-stable ratio of the secondary isotopes plays another important role to constrain the CR propagation. The unstable nuclei with lifetimes comparable to the diffusion time of the CRs, such as ^{10}Be ($\tau = 1.39 \times 10^6$ yr) and ^{26}Al ($\tau = 7.17 \times 10^5$ yr), can be used as the clocks to measure the residual time of CRs in the Milky Way halo.

Many works have been dedicated to using the secondary-to-primary ratios and the unstable-to-stable isotope ratios to constrain the CR propagation parameters (see, e.g., [6,9,12–19]). However, due to the large number of the model parameters and the degeneracy between different parameters, the investigation of the parameter space is incomplete and the conclusion might be biased. In addition, more and more data have been accumulated. It is necessary to combine different data sets in a statistical way. Recently several works employed the Markov chain Monte Carlo (MCMC) method to try to take a full scan of the parameter space with large samples of the data [20–26]. The MCMC method is known to be efficient for the minimization of the high-dimensional problem and is widely used in different areas.

We have developed a tool, `CosRayMC`, through embedding the CR propagation code in the MCMC sampler [27],

*Corresponding author.
yuanq@pmo.ac.cn
†Corresponding author.
bixj@ihep.ac.cn

which has already been applied to the study of the CR lepton excesses [28–33]. In light of the newly reported CR nuclei and B/C data by PAMELA and AMS-02, we apply this tool to revisit the CR propagation and constrain the propagation parameters in this work. Compared with previous studies [22–26], we present an extensive study of different propagation models, including the plain diffusion scenario, the diffusion reacceleration scenario, and the diffusion convection scenario. Furthermore, we employ a phenomenological treatment of the time-dependent solar modulation based on the solar activities. Finally, the predicted positron and antiproton fluxes of different propagation models are compared with the data as a consistency check.

This paper is organized as follows. In Sec. II we define the propagation model configurations. In Sec. III we describe the fitting procedure. The fitting results and expectations of secondary positron and antiproton fluxes are presented in Sec. IV. We discuss our results in Sec. V, and finally conclude in Sec. VI.

II. PROPAGATION MODELS

Galactic CRs are accelerated in cosmic accelerators such as supernova remnants and pulsars before they are injected into the ISM. During their propagation in the galaxy, secondary particles can be produced by the collisions between primary CRs and the ISM. The propagation of CRs in the Galaxy is usually described by the diffusive transport equation

$$\frac{\partial \psi}{\partial t} = Q(\mathbf{x}, p) + \nabla \cdot (D_{xx} \nabla \psi - \mathbf{V}_c \psi) + \frac{\partial}{\partial p} p^2 D_{pp} \frac{\partial}{\partial p} \frac{1}{p^2} \psi - \frac{\partial}{\partial p} \left[\dot{p} \psi - \frac{p}{3} (\nabla \cdot \mathbf{V}_c \psi) \right] - \frac{\psi}{\tau_f} - \frac{\psi}{\tau_r},$$

where ψ is the differential density of CR particles per momentum interval, Q is the source term, D_{xx} is the spatial diffusion coefficient, $\mathbf{V}_c$ is the convective velocity, D_{pp} is the diffusion coefficient in the momentum space describing the reacceleration effect, $\dot{p} \equiv \mathrm{d}p/\mathrm{d}t$ is the momentum loss rate, and τ_f and τ_r are correspondingly the time scales for nuclear fragmentation and radioactive decay.

The diffusion coefficient is usually assumed to vary with rigidity by a power-law form

$$D_{xx} = D_0 \beta^\eta \left(\frac{R}{R_0} \right)^\delta, \quad (1)$$

where D_0 is the normalization factor, R_0 is a reference rigidity, δ is the power-law index that depends on the property of turbulence in the ISM, β is the velocity in units of light speed, and η is a phenomenological parameter describing the velocity dependence of the diffusion coefficient at low energies, which is generally thought to be 1. For the single power-law form of D_{xx}, we fix R_0 to be 4 GV. For the broken power-law case (see below), R_0 is left to be free in the fitting.

TABLE I. Data taking time of various measurements and the average modeled sunspot numbers one year before the data taking time.

	Time	$\bar{N}$
ACE(^{10}Be/^{9}Be)	08/1997-04/1999	23.5
ACE(B/C)	05/2011-05/2016	54.3
PAMELA-2006(p)	11/2006	17.4
PAMELA-2007(p)	12/2007	7.3
PAMELA-2008(p)	12/2008	3.0
PAMELA-2009(p)	12/2009	1.0
AMS-02(p)	05/2011-11/2013	40.8
AMS-02(B/C)	05/2011-05/2016	54.3
PAMELA($\bar{p}$)	07/2006-12/2008	10.0
AMS-02(e^+)	05/2011-11/2013	40.8
AMS-02($\bar{p}$)	05/2011-05/2015	51.5

Note: the data below the middle line are not fitted.

We assume the convection velocity linearly and continuously vary from the galactic disk to halo, $\mathbf{V}_c = \mathbf{z} \cdot \mathrm{d}V_c/\mathrm{d}z$, where $\mathbf{z}$ is the position vector in the vertical direction to the galactic disk. Such a form can avoid the discontinuity at the galactic plane.

The reacceleration effect leads to a diffusion in the momentum space. Its diffusion coefficient in momentum space, D_{pp}, is related with the spatial diffusion coefficient as [34]

$$D_{pp} D_{xx} = \frac{4 p^2 v_A^2}{3\delta(4-\delta^2)(4-\delta)\omega}, \quad (2)$$

where the v_A is the Alfven velocity and ω is the ratio of magnetohydrodynamic wave energy density to magnetic field

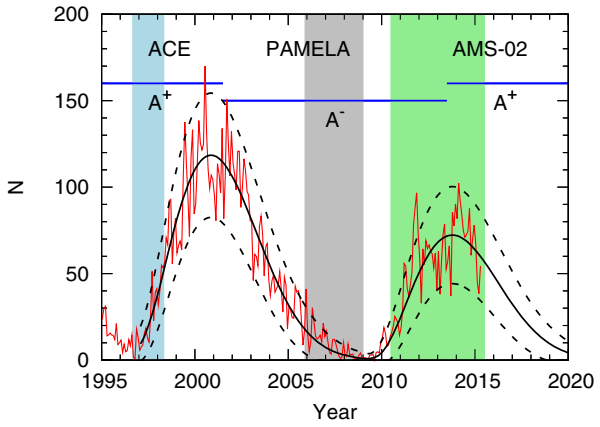

FIG. 1. Evolution of the sunspot numbers with time. The solid and dashed lines show the predicted sunspot numbers and the 95% intervals according to the monitored data [60]. Shaded regions show the periods of data taking (shifted leftwards by one year considering the possible delay of modulation effect compared with the solar activity) by ACE (for ^{10}Be/^{9}Be), PAMELA (for protons), and AMS-02 (for all species) detectors.

energy density. Since ω can be effectively absorbed in v_A, we assume it to be 1.

The source function $Q(\mathbf{x}, p)$ is expressed as $f(\mathbf{x})q(p)$, where $f(\mathbf{x})$ is the spatial distribution and $q(p)$ is the injection energy spectrum of CR sources. The spatial distribution is assumed to follow that of supernova remnants

$$f(r,z) = \left(\frac{r}{r_\odot}\right)^{1.25} \exp\left(-3.56 \cdot \frac{r-r_\odot}{r_\odot}\right) \exp\left(-\frac{|z|}{z_s}\right), \tag{3}$$

with parameters slightly adjusted to match the galactic diffuse γ-ray emission and the ratio of H_2 to CO [2,22]; $r_\odot = 8.5$ kpc is the distance from the Sun to the Galactic center; $z_s \approx 0.2$ kpc is the characteristic height of the galactic disk. The nuclei injection spectrum is assumed to be a broken power-law function of rigidity

$$q(R) \propto \begin{cases} (R/R_{\rm br})^{-\nu_1}, & R < R_{\rm br} \\ (R/R_{\rm br})^{-\nu_2}, & R \geq R_{\rm br} \end{cases}. \tag{4}$$

The power-law form of particle spectrum is expected from the simple shock acceleration mechanism. However, it has been found that the single power-law spectrum is somehow not enough to describe the observational data, especially when there is strong reacceleration of CRs [22]. The observations of γ-ray emission from a few supernova remnants that are interacting with molecular clouds also suggest a broken power law of CRs in or around the source [35]. Note that we neglect the potential second break at hundreds of GV of the CR nuclei [36–40], which is beyond the energy range we are interested in. Since we focus on the B/C ratio, the small difference between the spectra of protons and heavier nuclei [38,40] is also neglected.

The diffusive nature of charged particles in the Milky Way has been well established [1]. However, whether the reacceleration and/or convection plays significant roles in regulating the propagation of CRs is unclear. The widely existing galactic winds suggest that convective transport of CRs may be relevant [41]. On the other hand, the observed peak of the B/C around ~1 GeV/n by HEAO-3 [42] may require an effective reacceleration [43]. While the reacceleration model can fit the B/C data, it would underpredict antiprotons [43]. An adjustment of the η parameter in the diffusion coefficient was introduced to solve such a discrepancy [18]. The modification of the low energy diffusion coefficient is also physically motivated from the potential resonant interaction of CR particles and the magnetohydrodynamic (MHD) waves that results in dissipation of such waves [44].

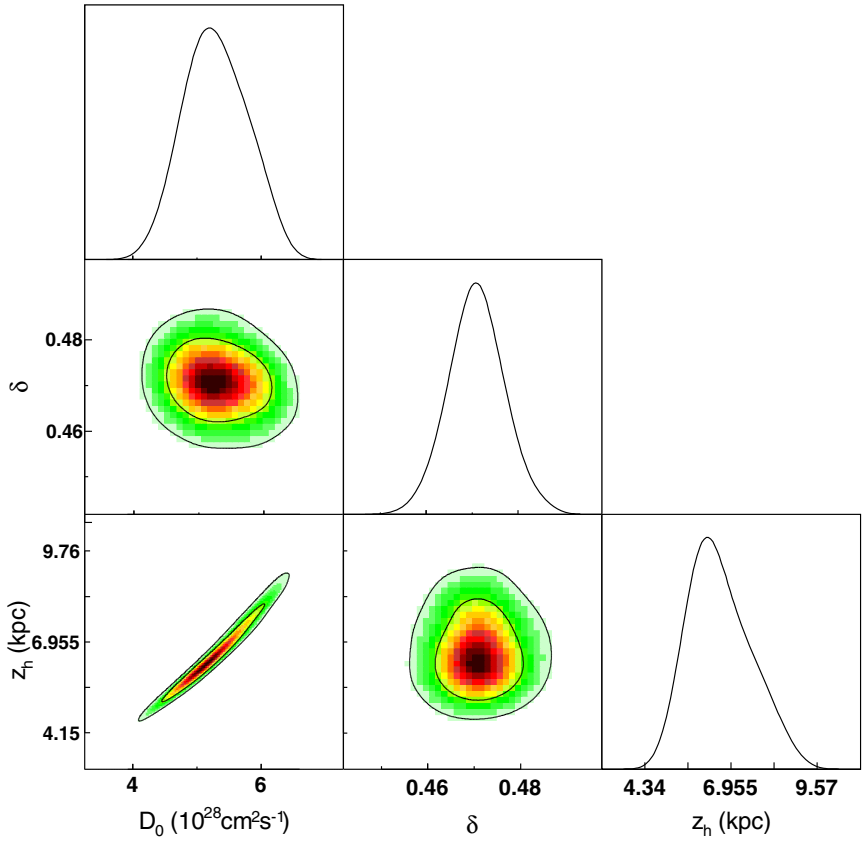

FIG. 2. Fitting 1D probability distributions and 2D credible regions (68% and 95% credible levels from inside to outside) of the model parameters in the PD scenario.

In this work we test all these kinds of models with the new observational data. Specifically, the propagation models include (1) the plain diffusion (PD) model without reacceleration and convection, (2) the diffusion convection (DC) model, (3) the diffusion convection model with a break of the rigidity dependence of the diffusion coefficient (with $\delta = 0$ below the break rigidity R_0 [43]; DC2), (4) the diffusion reacceleration (DR) model, (5) the diffusion reacceleration model with η left free to fit (DR2), and (6) the diffusion reacceleration convection (DRC) model. The relevant propagation parameters are $(D_0, \delta, z_h, v_A, dV_c/dz, R_0, \eta)$.

We keep in mind that the above described propagation framework is actually simplified. The diffusion coefficient may vary in the Milky Way due to different magnetic field distributions in the disk and halo (e.g., [45,46]). In particular, CRs may be confined much longer around the sources than expected due to nonlinear self-generation of MHD waves via streaming instability [47]. These complications are less clear and beyond the scope of the current work. The caveat is that considering these effects may result in different results from the adopted framework (see, e.g., [26]).

III. FITTING PROCEDURE

A. CosRayMC

The CosRayMC code is a combination of the numerical propagation code GALPROP [48] [9,10] and the MCMC sampler (adapted from CosmoMC [27]). The MCMC technique is widely applied in astrophysics and cosmology to investigate the high-dimensional parameter space from observational data. It works in the Bayesian framework. The posterior probability of model parameters $\boldsymbol{\theta}$ in light of the observational data D is $\mathcal{P}(\boldsymbol{\theta}|D) \propto \mathcal{P}(D|\boldsymbol{\theta})\mathcal{P}(\boldsymbol{\theta})$, where $\mathcal{P}(D|\boldsymbol{\theta})$ is the likelihood and $\mathcal{P}(\boldsymbol{\theta})$ is the prior probability of $\boldsymbol{\theta}$.

The Markov chain is generated following the Metropolis-Hastings algorithm. The general process is as follows. One first proposes a random step in the parameter space. Then the

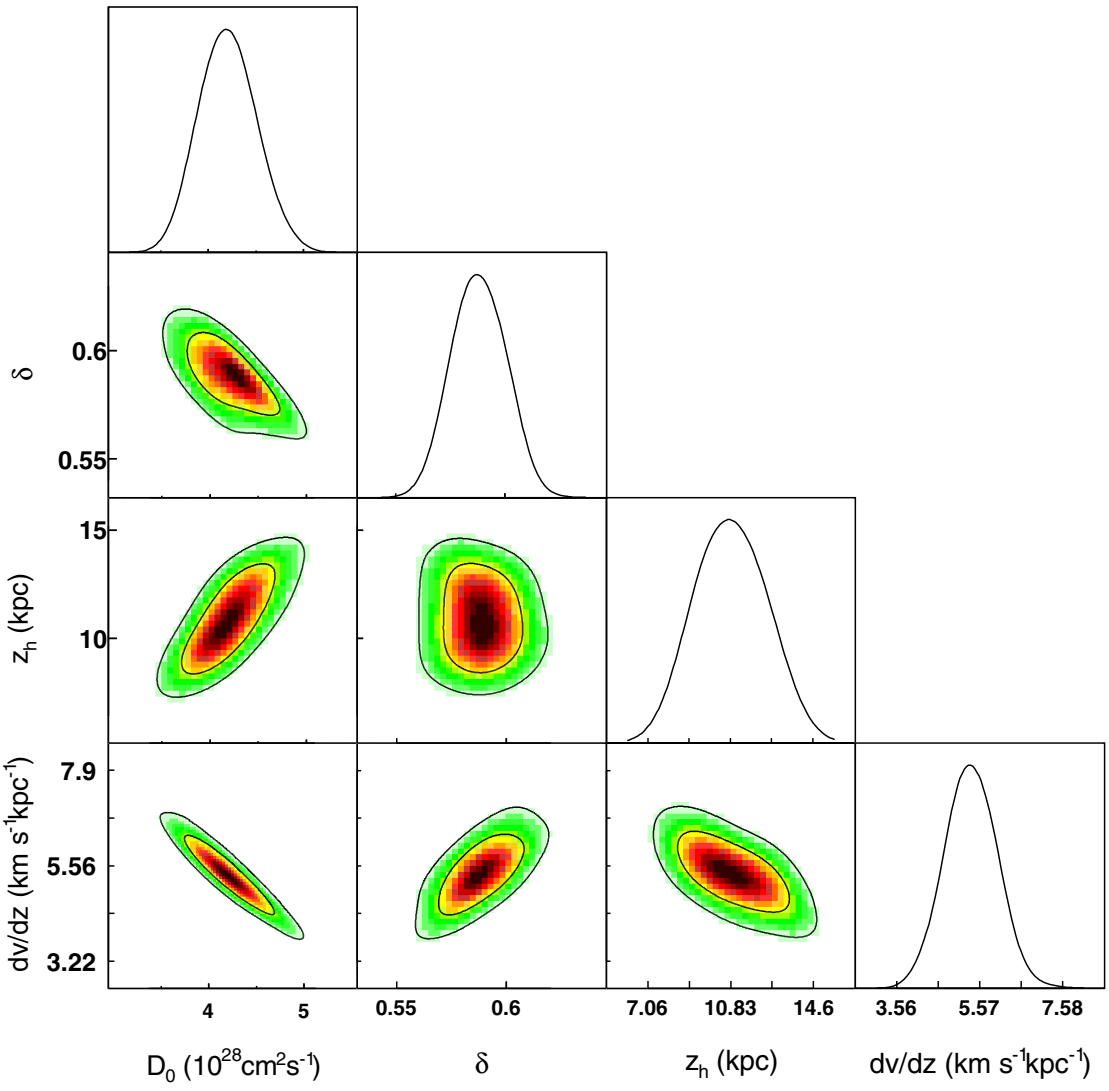

FIG. 3. Same as Fig. 2 but for the DC scenario (adding one more parameter, dV_c/dz).

acceptance probability is calculated by the ratio of the target probabilities of this proposed point to the former one. If the proposed point is accepted, then repeat this procedure. Otherwise, go back to the former point and have another trial. The stationary distribution of the chain samples approaches the target probability distribution $\mathcal{P}(\boldsymbol{\theta}|D)$. For more details, one can refer to [49,50].

B. Data sets

We adopt the most recently available accurate data sets of CRs by PAMELA and AMS-02 in our fittings. For the B/C ratio, we employ the just-released data by AMS-02, which cover an energy range of hundreds of MeV/n to TeV/n [51]. In order to have better constraints on the low energy behavior of the B/C ratio, we also employ the data from ACE-CRIS [52] with the same period as that of AMS-02. To constrain the lifetime of CRs in the Galaxy, we also use the $^{10}\mathrm{Be}/^{9}\mathrm{Be}$ data from some old measurements: Ulysses [53], ACE [14], Voyager [54], IMP [55], ISEE-3 [55], and ISOMAX [56]. The proton fluxes are employed to constrain the injection parameters of CRs. As is discussed in the next subsection, we try to give a more reasonable treatment of the solar modulation effect, the time-dependent proton fluxes from 2006 to 2009 measured by PAMELA [57], and the average flux from 2011 to 2013 by AMS-02 [39] is used. Table I summarizes the observational time of each data set.

C. Solar modulation

In this work we use the force-field approximation to account for the solar modulation of low energy CRs when propagating in the heliosphere [58]. However, since the various data sets in our work cover a wide time window in which solar activities vary much, they should not share a common modulation potential. Figure 1 shows the sunspot numbers of different time from 1995 to the present [59].

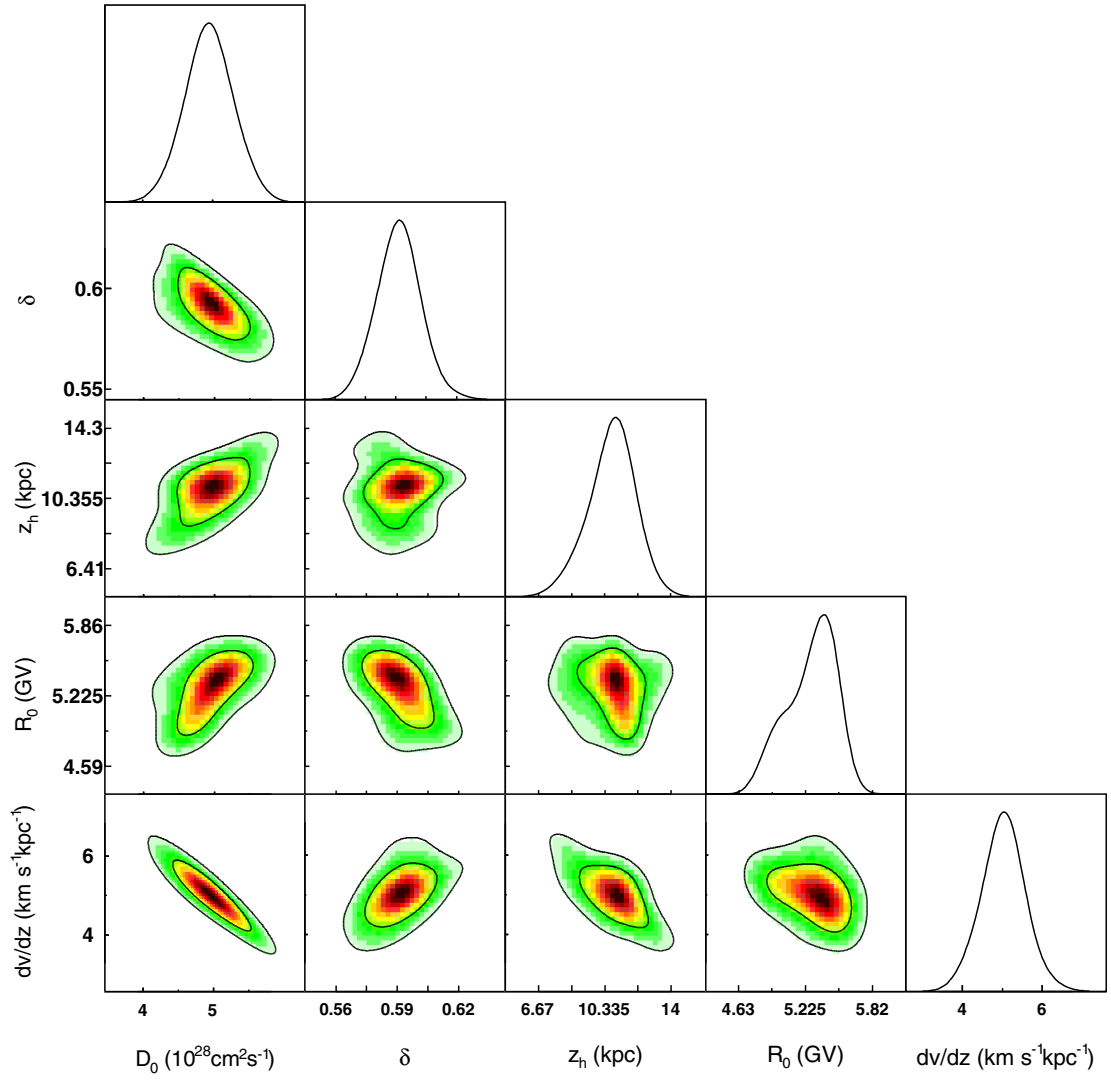

FIG. 4. Same as Fig. 2 but for the DC2 scenario (adding two more parameters, dV_c/dz and R_0).

The data we use are basically from the end of solar cycle 23 to the beginning of solar cycle 24, except for the $^{10}\mathrm{Be}/^{9}\mathrm{Be}$ data. More importantly they are roughly in the period that the polarity of the solar magnetic field is in the same A^- cycle. This enables us to have a relatively simple approach of the solar modulation with a correlation with solar activities.

Here we employ a linear evolution behavior of the modulation potential with respect to the evolution of the sunspot number

$$\Phi = \Phi_0 + \Phi_1 \times \frac{N(t)}{N_{\max}}, \tag{5}$$

where $N_{\max} \approx 72.2$ is the model predicted maximum sunspot number in solar cycle 24 (shown by the solid line in Fig. 1; [60]), $N(t)$ is the sunspot number during which the data were collected, and Φ_0 and Φ_1 are free parameters that are derived through fitting to the CR data. The average sunspot numbers for various CR data taking time are given in Table I. Note that we always count the sunspot number for the time *one year* before the actual data taking time, due to the possible delay of the modulation effect compared with solar activity. This treatment is consistent with the fact that the PAMELA proton flux in 12/2009 is higher than that in 12/2008, while the solar minimum of cycle 23 ended at the beginning of 2009. Given a typical speed of ~500 km/s, solar winds need about one year to fill the heliosphere with a scale of ~100 astronomical units, which further supports our treatment.

IV. RESULTS

A. Fitting results of various models

We use the MCMC algorithm to determine the model parameters of the six models as described in Sec. II through fitting to the data. The posterior mean and 68% credible uncertainties of the model parameters are given in Table II. Since the data are precise enough, we obtain *statistically* good constraints on the model parameters. Some of the model parameters, such as the injection spectral indices, are

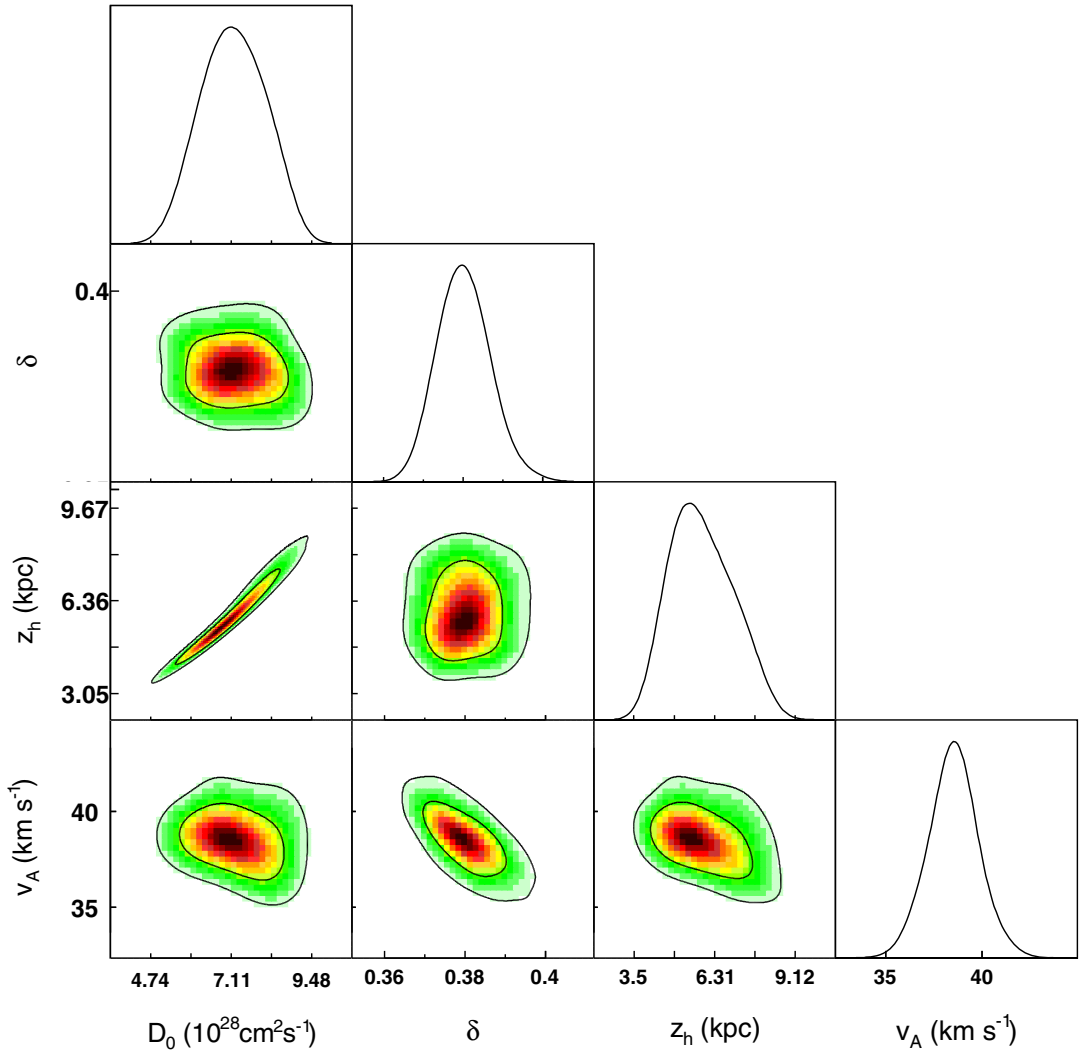

FIG. 5. Same as Fig. 2 but for the DR scenario (adding one more parameter, v_A).

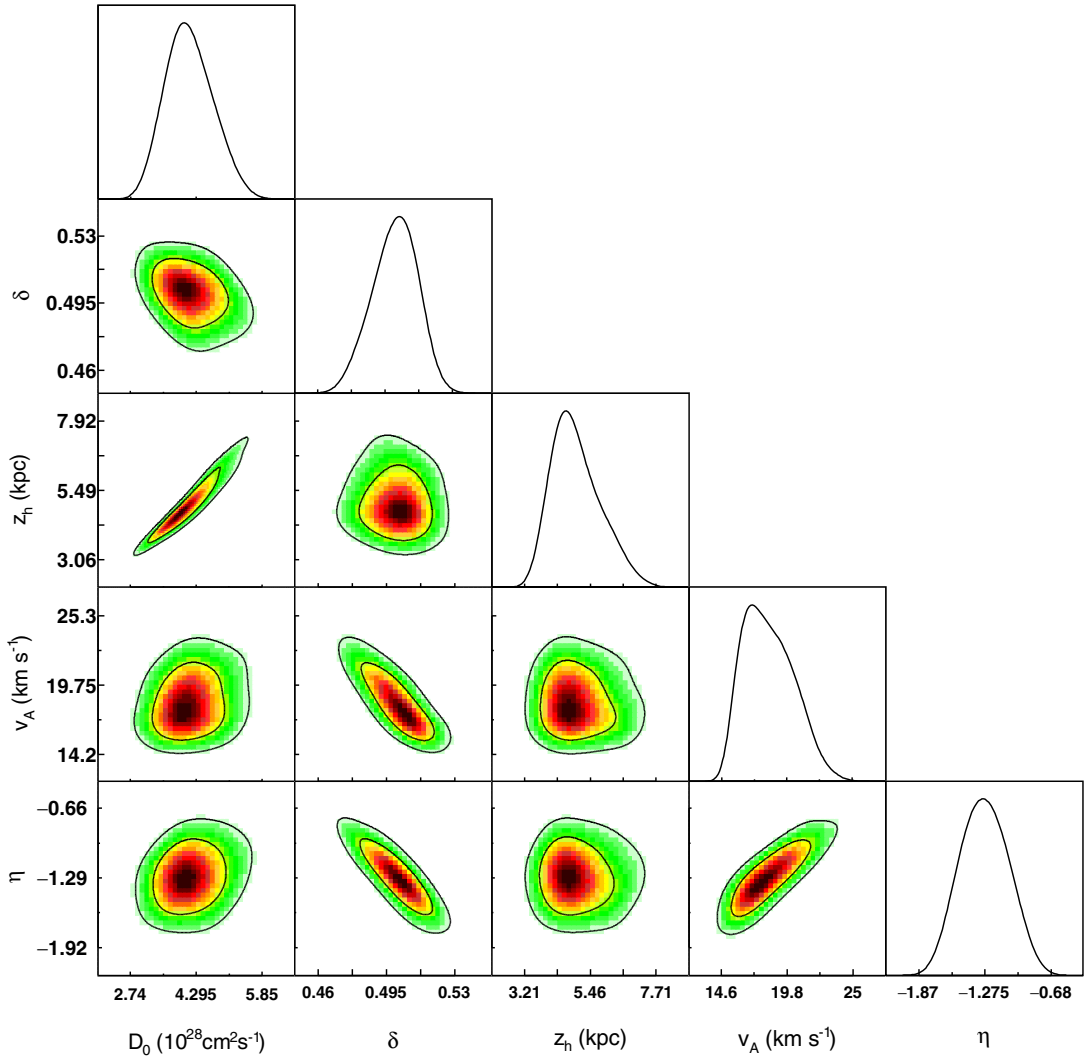

FIG. 6. Same as Fig. 2 but for the DR2 scenario (adding two more parameters, v_A and η).

constrained to a level of $\lesssim 1\%$. The propagation parameters are constrained to be about 10%–20%, which are relatively large due to the degeneracy among some of them. For the rigidity-dependent slope of the diffusion coefficient, δ, the statistical error is only a few percent. Compared with previous studies [22–24], our results are widely improved. The one-dimensional (1D) probability distributions and two-dimensional (2D) confidence regions of the major propagation parameters are summarized in Figs. 2–7. We also show explicitly the comparison of the data with the fitting results (with 95% credible bands) in Figs. 8–10.

The fittings show that the models with reacceleration (DR, DR2, and DRC) can fit the B/C and proton data well, while the other three nonreacceleration models fit the data relatively poorly.[1] The reduced chi-squared values are all smaller than 1 for the three reacceleration models. For the nonreacceleration models, the χ^2 values indicate p values of $\sim 7.8 \times 10^{-16}$, 4.3×10^{-5}, and 0.14 for the PD, DC, and DC2 models, respectively. From Fig. 8 we can see that the predicted B/C ratios for nonreacceleration models do not match the low energy ($E_k \lesssim 1$ GeV/n) data well. This is perhaps due to larger solar modulation potentials for nonreacceleration models, which are required by the proton data. These results illustrate the importance of including the low energy ACE data of B/C and the primary CR flux data when studying the propagation of CRs.

There is a clear degeneracy between D_0 and z_h. This is because the B/C data can only constrain D_0/z_h effectively [6,23]. The unstable-to-stable secondary ratio is expected to break such a degeneracy. However, the current $^{10}\mathrm{Be}/^{9}\mathrm{Be}$ ratio data are of relatively poor quality. The 95% credible region of D_0 is $[5.2, 9.2] \times 10^{28}$ cm^2 s^{-1} for the DR model, and the corresponding value of z_h is [3.7, 8.2] kpc. As a comparison, they are $[5.45, 11.20] \times 10^{28}$ cm^2 s^{-1}, and [3.2, 8.6] kpc in

[1]Note, however, that the study of CR electrons and positrons results in a different conclusion, i.e., the convection models are more favored than the reacceleration models [62].

Ref. [22]. Our results improve moderately compared with that of Ref. [22]. Through analyzing the synchrotron radiation and the electron/positron fluxes, Di Bernardo *et al.* also found a relatively large propagation halo height ($z_h > 2$ kpc; [63]), which is consistent with our results.

There are some other correlations among the propagation parameters. For example, for the DC and DC2 scenario, an anticorrelation between D_0 and dV_c/dz can be found (Figs. 3 and 4). It can be understood that a larger convection velocity tends to blow the particles away from the disk, resulting in a lower flux, which can be compensated by a longer propagation time (hence a smaller D_0). A positive correlation between δ and dV_c/dz can be understood similarly. Since the convection is only important for low energy particles, a larger convection velocity leads to harder spectra of the CR fluxes and B/C ratio, which can be compensated by a larger value of δ. For the DR2 scenario, we find anticorrelations between v_A and δ, η, and δ, and positive correlation between v_A and η. A larger v_A value gives softer spectra of the CR fluxes and B/C ratio, hence suggesting a smaller δ. The anticorrelation between η and δ can be understood as a smaller η (note that $\eta < 0$) giving a larger diffusion coefficient at low energies, and resulting in harder spectra after the propagation. A larger value of δ is then able to compensate such an effect.

The slope δ of the diffusion coefficient is well constrained (with statistical uncertainty of a few percent) given the model setting. However, there are relative large differences among different model configurations. For the reacceleration models, δ is about 0.38 for the DR model, and about 0.5 for the DR2/DRC models. For the DC/DC2 models, δ is even larger (about 0.6). These results can be understood via the correlations between δ and other parameters as described above. The fitting to the B/C ratio above 65 GV gives a slope of -0.333 [51]. Our results show that in specific models the value of δ may differ from that directly inferred from the data. This is because, on one hand, the low energy spectrum of the B/C ratio depends on propagation models, and on the other hand, the uncertainties of high energy data are relatively large. It is currently difficult to distinguish the

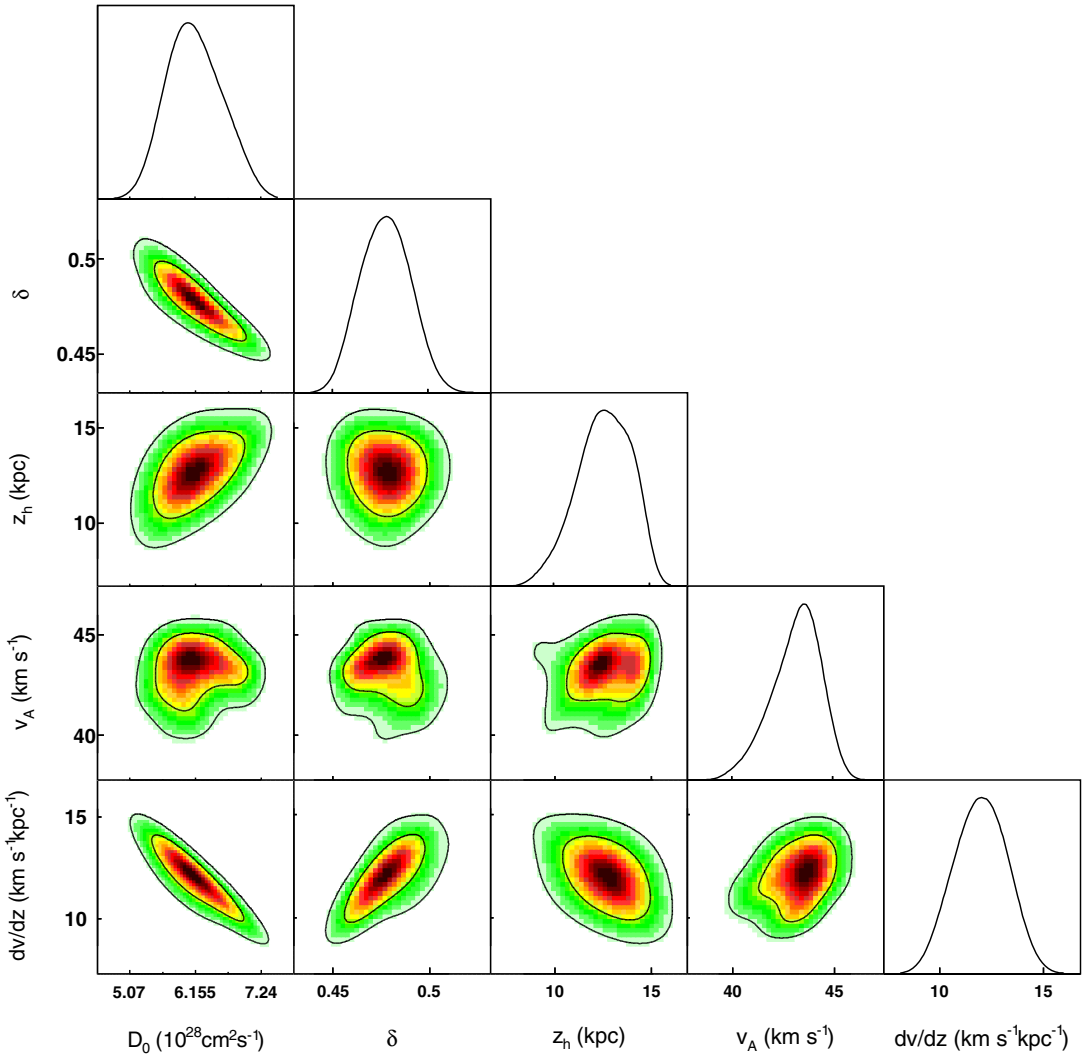

FIG. 7. Same as Fig. 2 but for the DRC scenario (adding two more parameters, v_A and dV_c/dz).

Kolmogrov ($\delta = 1/3$; [64]) and the Kraichnan ($\delta = 1/2$; [65]) type of interstellar turbulence. Nevertheless, we find that for some of the propagation model settings, such as the DR2 and DRC models, the Kraichnan type of turbulence is favored. For the DR model, the fitting value of δ is closer to, but still different from, that predicted by the Kolmogrov theory.

For reacceleration models, the Alfven velocity v_A is about 38 $\mathrm{km\,s^{-1}}$ for the DR model, which decreases (increases) to about 18 (43) $\mathrm{km\,s^{-1}}$ for the DR2 (DRC) model. The major effect of reacceleration is to produce a "GeV bump" of the CR flux and B/C ratio. For the DR2 model, a larger δ gives a higher B/C ratio at lower energies, and hence a smaller reacceleration effect is needed. This can also be seen from the anticorrelation between v_A and δ (Fig. 6). The effect of convection is, however, opposite from that of reacceleration. Therefore for the DRC model, a larger value of v_A is favored given a nonzero value of dV_c/dz.

A break of the injection spectrum around 10–20 GV is favored in the reacceleration models. Such a break is required to fit the proton fluxes, in order to reduce the GeV bump produced by the reacceleration. Such a break is not necessary for the nonreacceleration models. Nevertheless, we find that a spectral hardening with a change of the slope of ~0.10−0.15 is favored by the fitting.

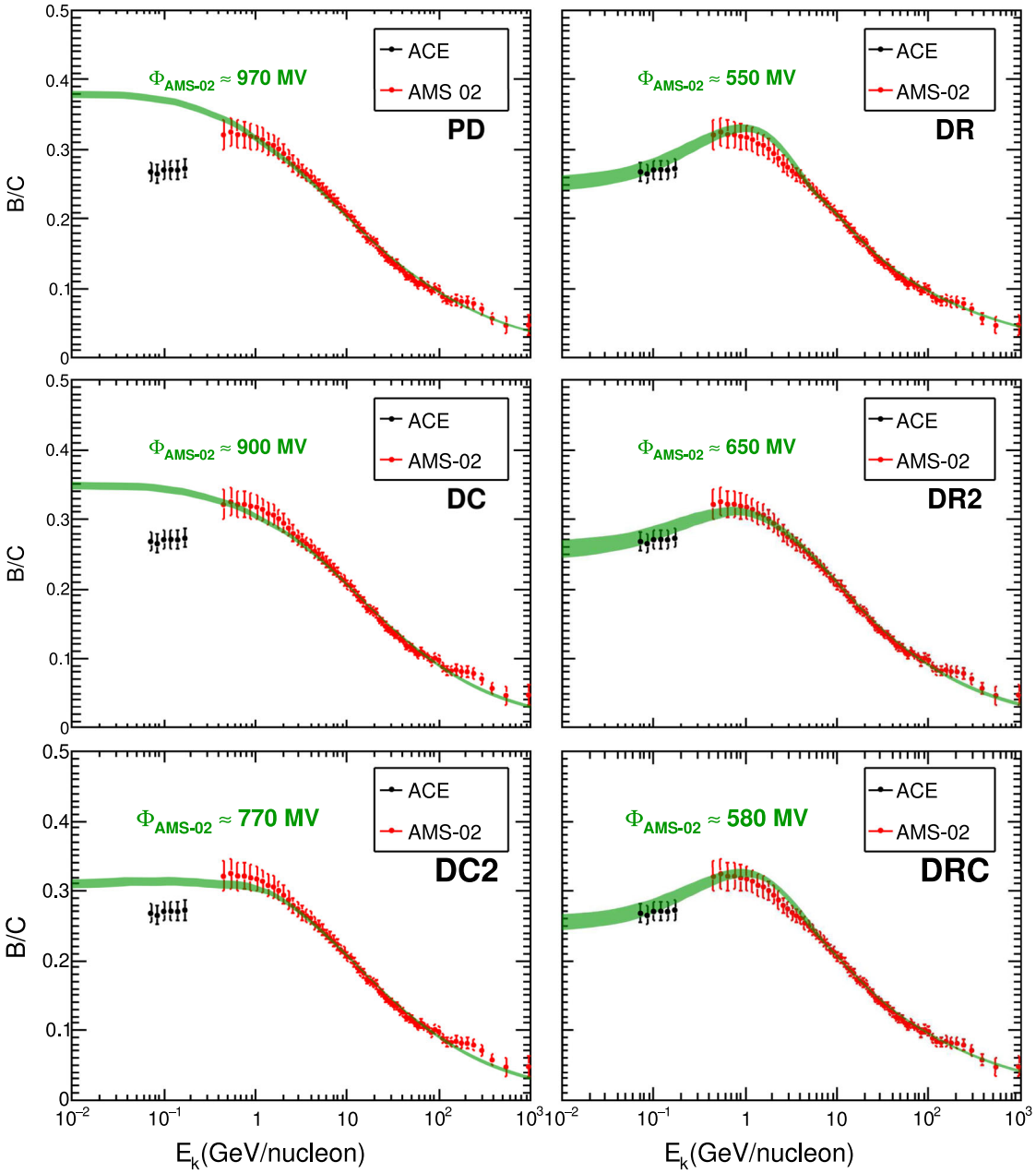

FIG. 8. 2σ bands of the B/C ratios for different PD propagation models. The observational data are from ACE [61] and AMS-02 [51].

Such a break enables a better fit to the high energy proton flux by the AMS-02, which shows a spectral hardening above ~330 GV. The break rigidity is not exactly the same as that obtained directly from the data, because the low energy spectral behavior also enters in the fitting.

As for the solar modulation, we find that the time-dependent term of the modulation potential, Φ_1, is similar for all models. It reflects the differences of the proton fluxes at different time. The platform terms Φ_0 differ from each other. In general, nonreacceleration models need remarkably larger Φ_0 to accommodate the low energy data of protons.

B. Positrons

The fluxes of secondary positrons can be calculated self-consistently given the fitting propagation and source parameters. Figure 11 shows the expected 2σ bands of positron fluxes, compared with the AMS-02 data [66]. We find that the reacceleration models that fit the B/C and proton data well result in a remarkable bump at ~GeV energies and exceed the data significantly. This is consistent with that found in earlier studies [22,43]. For the nonreacceleration models, on the other hand, the expected positron fluxes are lower than the data by a factor of ~2–3. These results

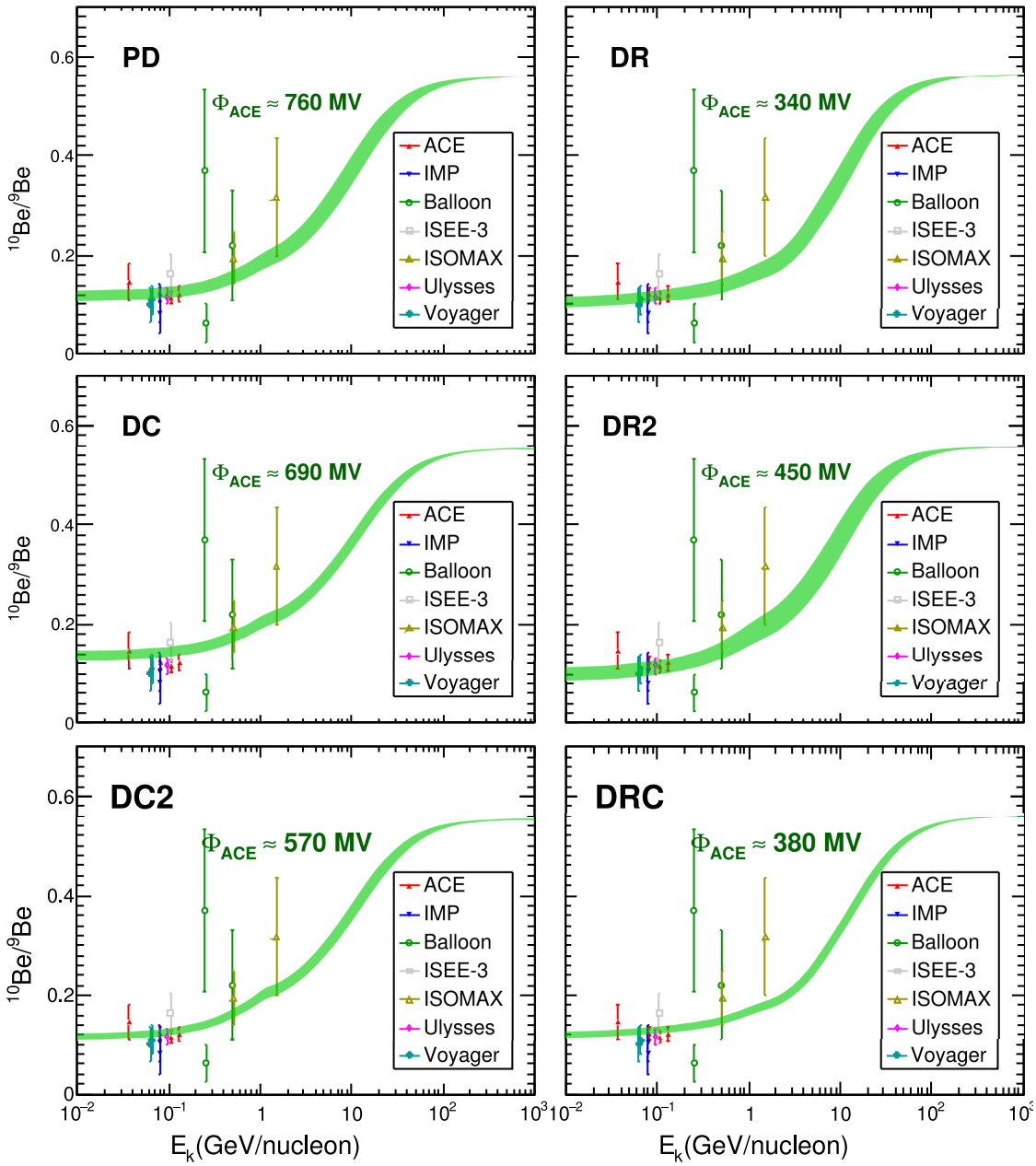

FIG. 9. 2σ bands of the ^{10}Be/^{9}Be ratios for different propagation models. The observational data are from Ulysses [53], ACE [14], Voyager [54], IMP [55], ISEE-3 [55], and ISOMAX [56].

indicate that the production and propagation of positrons may be significantly different from that of the CR nuclei.

For all these models, the predicted positron spectra at high energies ($\gtrsim$10 GeV) are much softer than that of the data, which indicate the existence of primary positron sources, e.g., pulsars [67–69].

C. Antiprotons

Figure 12 shows the results of antiprotons from the models, compared with the PAMELA [70] and AMS-02 [71] measurements. We find that the model predictions are roughly consistent with the data. More detailed comparison shows that in general the nonreacceleration model predictions match the data better than the reacceleration models. For the DR and DRC models, there are slight deficits of low energy ($\lesssim$10 GeV) antiprotons compared with the data. The DR2 model can marginally fit the data. The prediction of the DC2 model is consistent with the data. For the PD and DC models, however, they slightly underpredict antiprotons around 10 GeV and overpredict lower energy antiprotons. At the high energy end ($E \gtrsim 100$ GeV), there might be excesses of the data (see also [72–75]). For models with larger δ values such as the DC, DC2, and DR2 models, the excesses are remarkable. For the other three

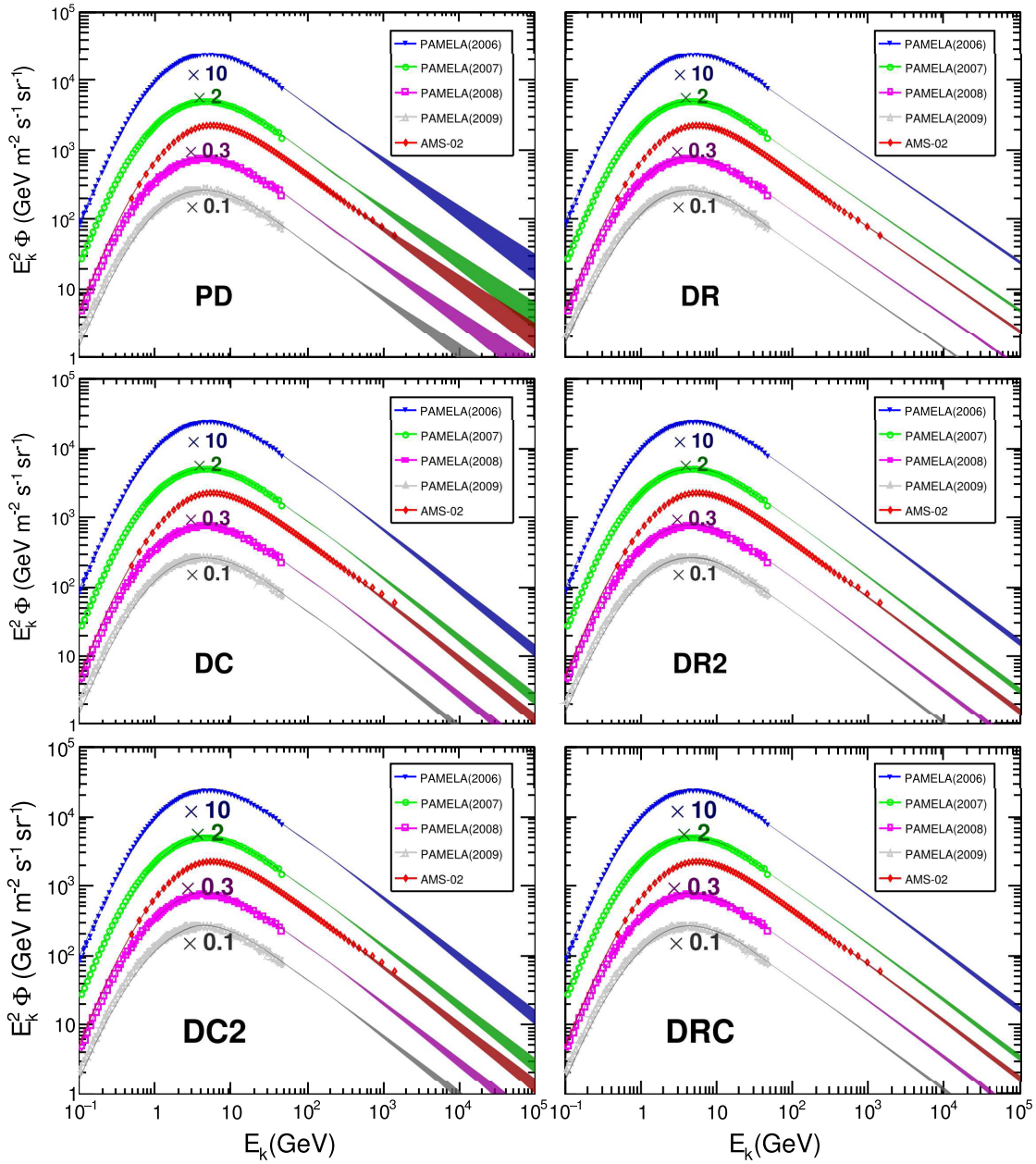

FIG. 10. Fitting 2σ bands of the proton spectra, compared to the PAMELA results at four different epochs [57] and the AMS-02 data [39].

models with relatively smaller δ values such excesses are less significant.

V. DISCUSSION

A. The discrepancy between nonreacceleration models and CR nuclei data

It seems that the nonreacceleration models have difficulty fitting the proton fluxes and the B/C ratio simultaneously. We find that for the nonreacceleration models the required solar modulation potential (Φ_0) is significantly higher than that of reacceleration models, which results in poor fittings to the low energy B/C data of ACE. To test that whether such a discrepancy is due to the difference of solar modulation between protons and heavy nuclei, we do similar fittings using the preliminary carbon flux by AMS-02 [76] instead of the proton fluxes. We find similar conclusion as above, which means that the difference of solar modulation between protons and heavy nuclei is not the major reason of this discrepancy.

Another possible reason is the injection spectrum of CRs. For the three nonreacceleration models the injection spectrum at low rigidities is proportional to $R^{-(2.4-2.5)}$, which is quite soft compared with that of the reacceleration models $R^{-(1.7-2.0)}$. Even though we enable a break of the low energy spectrum of all the models, the fitting results turn out to favor a high energy hardening instead of a low energy break for the nonreacceleration models. We have added another break in the injection spectrum of Eq. (4), and redo the fittings. Still no effective improvement of the fittings is found.

B. The discrepancy between all models and the positron data

Our results show that the reacceleration models overpredict low energy (∼GeV) positrons compared with the measurements, while the nonreacceleration models tend to underpredict positrons. Similar results for reacceleration models have also been obtained in Ref. [63]. One kind of uncertainty is the hadronic pp-interaction. In this work we use the parametrization of positron production in pp-interaction of Ref. [77]. As illustrated in Ref. [78], some other parametrizations give a positron yield spectrum differing by a factor of $\lesssim 2$ in a certain energy range. However, the uncertainty of the hadronic interaction may not be able to fully solve this discrepancy, especially for the reacceleration models. The other models adopted in Ref. [78] give even more positrons between GeV and TeV, which makes the reacceleration models exceed the data even more. Therefore our results indicate that the propagation of CR nuclei and leptons, either in the Galaxy or in the heliosphere, might be different. Given the very efficient energy losses of leptons, they may experience large fluctuations in the Galaxy [79]. The solar modulation effects may also be different between nuclei and leptons due to their distinct mass-to-charge ratios. The charge-sign dependent solar modulation may take effect too [80–84].

C. The Voyager-1 measurements in the outer heliosphere

The Voyager-1 spacecraft has traveled more than 100 astronomical units from the Earth. It has been thought to approach the edge of the heliosphere since a sudden drop of the intensity of low energy ions and an abrupt increase of the CR intensity from outside the heliosphere were observed [85]. The measured CR flux by Voyager 1 can thus be believed to be a direct measurement of the local interstellar CRs. The Voyager-1 data would be helpful in better constraining the source injection parameters as well as the solar modulation parameters. However, as shown in Ref. [86], the very low energy ($\lesssim 50$ MeV/n) B/C spectrum

TABLE II. Posterior mean and 68% credible uncertainties of the model parameters.

	Unit	PD	DC	DC2	DR	DR2	DRC
D_0	$(10^{28}\ \mathrm{cm^2\ s^{-1}})$	5.29 ± 0.51	4.20 ± 0.30	4.95 ± 0.35	7.24 ± 0.97	4.16 ± 0.57	6.14 ± 0.45
δ		0.471 ± 0.006	0.588 ± 0.013	0.591 ± 0.011	0.380 ± 0.007	0.500 ± 0.012	0.478 ± 0.013
z_h	(kpc)	6.61 ± 0.98	10.90 ± 1.60	10.80 ± 1.30	5.93 ± 1.13	5.02 ± 0.86	12.70 ± 1.40
v_A	$(\mathrm{km\ s^{-1}})$	⋯	⋯	⋯	38.5 ± 1.3	18.4 ± 2.0	43.2 ± 1.2
dV_c/dz	$(\mathrm{km\ s^{-1}\ kpc^{-1}})$	⋯	5.36 ± 0.64	5.02 ± 0.55	⋯	⋯	11.99 ± 1.26
R_0	(GV)	⋯	⋯	5.29 ± 0.23	⋯	⋯	⋯
η		⋯	⋯	⋯	⋯	-1.28 ± 0.22	⋯
$\log(A_p)^a$		-8.334 ± 0.003	-8.334 ± 0.003	-8.336 ± 0.003	-8.347 ± 0.002	-8.334 ± 0.002	-8.345 ± 0.002
ν_1		2.44 ± 0.01	2.45 ± 0.01	2.43 ± 0.01	1.69 ± 0.02	2.04 ± 0.03	1.82 ± 0.02
ν_2		2.34 ± 0.03	2.30 ± 0.01	2.30 ± 0.01	2.37 ± 0.01	2.33 ± 0.01	2.37 ± 0.01
$\log(R_{br})^b$		5.06 ± 0.13	4.82 ± 0.05	4.78 ± 0.06	4.11 ± 0.02	4.03 ± 0.03	4.22 ± 0.03
Φ_0	(GV)	0.595 ± 0.005	0.537 ± 0.006	0.419 ± 0.005	0.180 ± 0.008	0.290 ± 0.014	0.220 ± 0.008
Φ_1	(GV)	0.495 ± 0.011	0.485 ± 0.011	0.472 ± 0.012	0.487 ± 0.011	0.485 ± 0.011	0.482 ± 0.013
χ^2/dof		748.6/463	591.0/462	494.6/461	438.8/462	341.0/461	380.5/461

[a]Propagated flux normalization at 100 GeV in units of $\mathrm{cm^{-2}\ s^{-1}\ sr^{-1}\ MeV^{-1}}$.
[b]Break rigidity of proton injection spectrum in units of MV.

measured by Voyager 1 is difficult to be modeled in various models. Further tuning of the modeling and/or better understanding about the measurements may be necessary. The Voyager-1 data are included in future studies.

D. Reacceleration models and antiprotons

The reacceleration models generally underestimate the low energy antiproton fluxes. Several kinds of scenarios were proposed to explain this. In Ref. [87] it was proposed that a local and fresh source, probably associated with the Local Bubble, might produce additional low energy primaries and hence decrease the measured secondary-to-primary nuclei ratio. The annihilation of several tens of GeV dark matter particles may also be responsible for the low energy excess of antiprotons [88–90]. Alternatively, an empirical adjustement of the velocity dependence of the diffusion coefficient with a β^{η} term, i.e., the DR2 model in this work, was suggested to be able to explain the B/C and antiproton data [18]. In this treatment a larger δ value and a weaker reacceleration effect is required, which enables more production of low energy secondary particles (both boron and antiprotons). As shown in Fig. 12, the DR2 model does improve the fitting. However, the physical motivation for such a term is not well justified. Finally, the uncertainties of the production cross section of antiprotons make this problem still inconclusive [91–93].

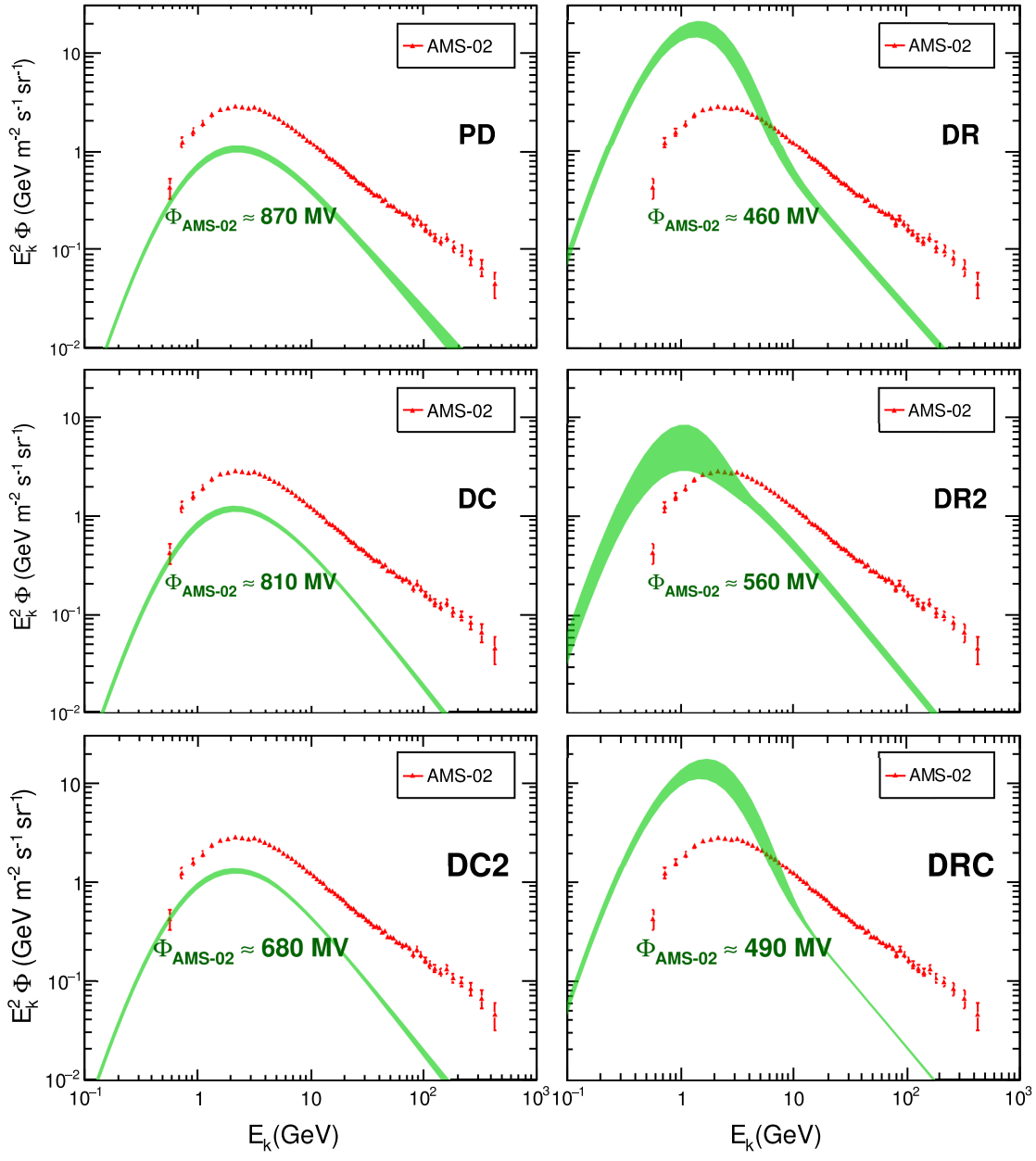

FIG. 11. Predicted 2σ bands of the positron spectra, compared with the AMS-02 measurements [66].

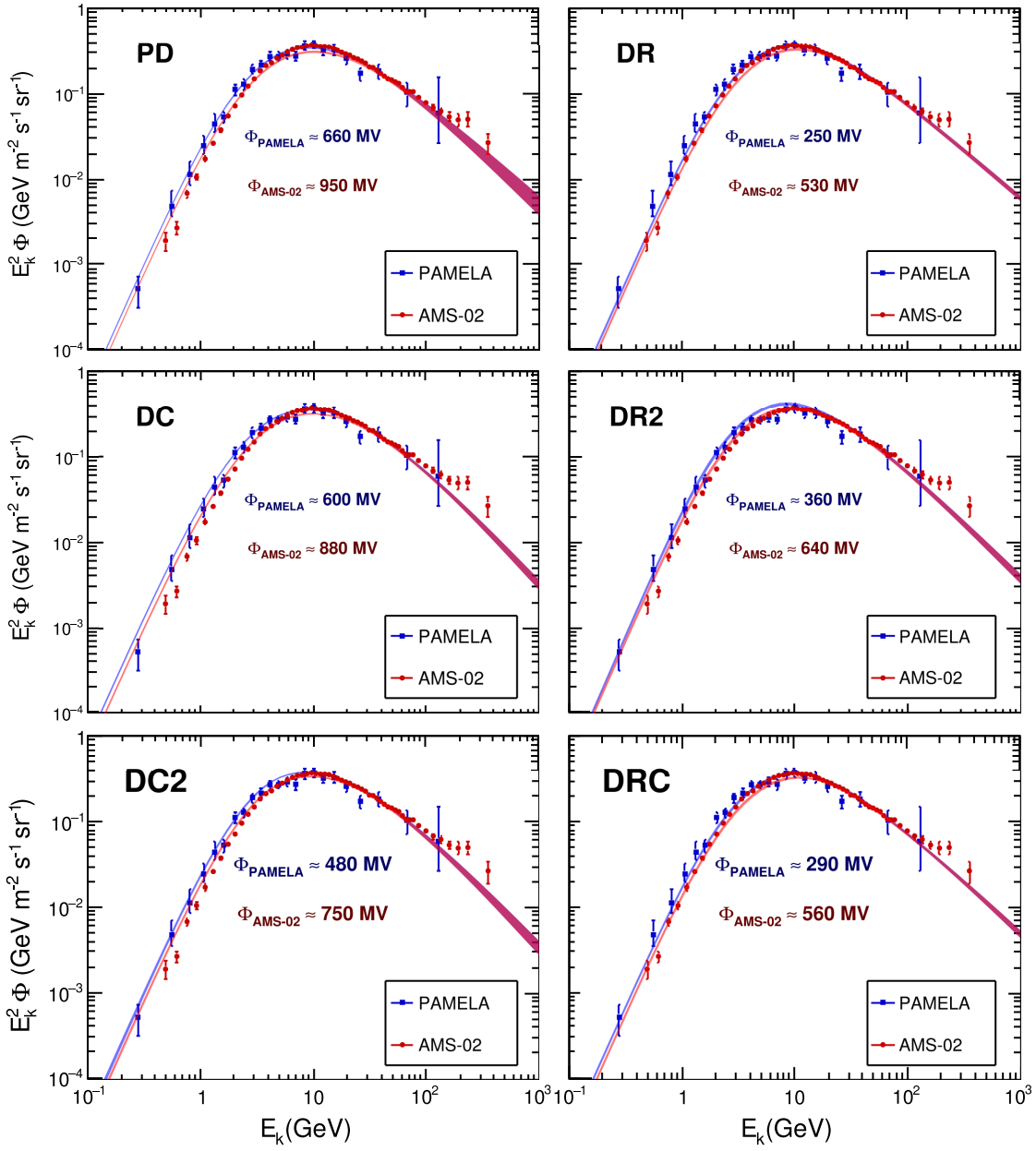

FIG. 12. Predicted 2σ bands of the antiproton spectra, compared with the PAMELA [70] and AMS-02 data [71].

VI. CONCLUSION

In this work we adopt the precise measurements of the B/C ratio and the time-dependent proton fluxes by AMS-02 and PAMELA to constrain the injection and propagation parameters of galactic CRs. We employ a self-consistent treatment of the solar modulation by means of a linear correlation of the modulation potentials with solar activities. We have carried out a comprehensive study of a series of CR propagation models, including the PD, DR, DC, DRC, and two variants of the DR and DC models. The predictions of secondary positrons and antiprotons based on the fitting parameters are calculated and compared with the data.

We summarize the comparison of various models with different data sets in Table III. It is shown that no model can match all these data simultaneously, which suggests that the actual case for the origin, propagation, and interaction of CRs is more complicated than our current understanding. For the CR nuclei only, we find that the DR2 model may give the best match to all the data. However, the phenomenological modification of the diffusion coefficient (the β^{η} term) may need to be understood further [18].

We list our main conclusion as follows.

(i) The reacceleration models (DR, DR2, and DRC) can fit both the B/C and proton fluxes well, while nonreacceleration models (PD, DC, and DC2)

TABLE III. Summary of different propagation models versus the data.

	B/C and protons	Positrons	Antiprotons
PD	Poor	Too few	Fair
DC	Poor	Too few	Fair
DC2	Poor	Too few	Good
DR	Good	Too many	Slightly few
DR2	Good	Too many	Fair
DRC	Good	Too many	Slightly few

cannot. The failure of nonreacceleration models cannot be simply ascribed to the differences of solar modulation or the source injection spectra between protons and heavier nuclei.

(ii) The statistical uncertainties of the propagation parameters are constrained to a level of 10%–20%, thanks to the precise measurements of CR data by AMS-02. However, there are relatively large differences (up to a factor of ∼2) among different model settings.

(iii) For reacceleration models, the value of δ is found to be about 0.38–0.50, which slightly favors the Kraichnan type of interstellar turbulence.

(iv) The reacceleration models overproduce positrons but underproduce (except DR2) antiprotons in general. The nonreacceleration models, on the other hand, predict fewer positrons and (marginally) consistent antiprotons when compared with the measurements.

(v) Our results suggest that there are significant differences of the propagation in either the Milky Way or the heliosphere between nuclei and leptons.

With more and more precise data available, we are able to investigate the CR-related problems in great detail. It turns out that the problem seems to be more complicated than what we expected based on the rough measurements in the past. The final understanding of the propagation of CRs may need not only the CR data themselves but also the full improvements of the understanding of the astrophysical ingredients of the Milky Way, as well as the nuclear and hadronic interactions.

ACKNOWLEDGMENTS

We thank the ACE CRIS instrument team and the ACE Science Center for providing the ACE data. This work is supported by the National Key Research and Development Program of China (Grant No. 2016YFA0400200), the National Natural Science Foundation of China (Grant No. 11475191), and the 100 Talents program of Chinese Academy of Sciences.

[1] T. K. Gaisser, *Cosmic Rays and Particle Physics* (Cambridge and New York, Cambridge University Press, 1990), p. 292.
[2] A. W. Strong, I. V. Moskalenko, and V. S. Ptuskin, Annu. Rev. Nucl. Part. Sci. **57**, 285 (2007).
[3] V. S. Berezinskii, S. V. Bulanov, V. A. Dogiel, and V. S. Ptuskin, *Astrophysics of Cosmic Rays*, edited by V. L. Ginzburg (North-Holland, Amsterdam, 1990).
[4] W. R. Webber, M. A. Lee, and M. Gupta, Astrophys. J. **390**, 96 (1992).
[5] J. B. G. M. Bloemen, V. A. Dogel, V. L. Dorman, and V. S. Ptuskin, Astron. Astrophys. **267**, 372 (1993).
[6] D. Maurin, F. Donato, R. Taillet, and P. Salati, Astrophys. J. **555**, 585 (2001).
[7] D. Maurin, R. Taillet, and F. Donato, Astron. Astrophys. **394**, 1039 (2002).
[8] T. Shibata, M. Hareyama, M. Nakazawa, and C. Saito, Astrophys. J. **612**, 238 (2004).
[9] A. W. Strong and I. V. Moskalenko, Astrophys. J. **509**, 212 (1998).
[10] I. V. Moskalenko and A. W. Strong, Astrophys. J. **493**, 694 (1998).
[11] C. Evoli, D. Gaggero, D. Grasso, and L. Maccione, J. Cosmol. Astropart. Phys. 10 (2008) 18.
[12] S. P. Swordy, D. Mueller, P. Meyer, J. L'Heureux, and J. M. Grunsfeld, Astrophys. J. **349**, 625 (1990).
[13] D. Mueller, S. P. Swordy, P. Meyer, J. L'Heureux, and J. M. Grunsfeld, Astrophys. J. **374**, 356 (1991).
[14] N. E. Yanasak *et al.*, Astrophys. J. **563**, 768 (2001).
[15] A. M. Lionetto, A. Morselli, and V. Zdravkovic, J. Cosmol. Astropart. Phys. 9 (2005) 10.
[16] M. Ave, P. J. Boyle, C. Höppner, J. Marshall, and D. Müller, Astrophys. J. **697**, 106 (2009).
[17] M. Pato, D. Hooper, and M. Simet, J. Cosmol. Astropart. Phys. 6 (2010) 22.
[18] G. di Bernardo, C. Evoli, D. Gaggero, D. Grasso, and L. Maccione, Astropart. Phys. **34**, 274 (2010).
[19] A. Obermeier, P. Boyle, J. Hörandel, and D. Müller, Astrophys. J. **752**, 69 (2012).
[20] A. Putze, L. Derome, D. Maurin, L. Perotto, and R. Taillet, Astron. Astrophys. **497**, 991 (2009).
[21] A. Putze, L. Derome, and D. Maurin, Astron. Astrophys. **516**, A66 (2010).
[22] R. Trotta, G. Jóhannesson, I. V. Moskalenko, T. A. Porter, R. Ruiz de Austri, and A. W. Strong, Astrophys. J. **729**, 106 (2011).
[23] H.-B. Jin, Y.-L. Wu, and Y.-F. Zhou, J. Cosmol. Astropart. Phys. 9 (2015) 049.

[24] G. Jóhannesson *et al.*, Astrophys. J. **824**, 16 (2016).
[25] M. Korsmeier and A. Cuoco, Phys. Rev. D **94**, 123019 (2016).
[26] J. Feng, N. Tomassetti, and A. Oliva, Phys. Rev. D **94**, 123007 (2016).
[27] A. Lewis and S. Bridle, Phys. Rev. D **66**, 103511 (2002).
[28] J. Liu, Q. Yuan, X. J. Bi, H. Li, and X. M. Zhang, Phys. Rev. D **81**, 023516 (2010).
[29] J. Liu, Q. Yuan, X. Bi, H. Li, and X. Zhang, Int. J. Mod. Phys. A **27**, 1250024 (2012).
[30] J. Liu, Q. Yuan, X.-J. Bi, H. Li, and X. Zhang, Phys. Rev. D **85**, 043507 (2012).
[31] Q. Yuan, X.-J. Bi, G.-M. Chen, Y.-Q. Guo, S.-J. Lin, and X. Zhang, Astropart. Phys. **60**, 1 (2015).
[32] Q. Yuan and X.-J. Bi, Phys. Lett. B **727**, 1 (2013).
[33] Q. Yuan and X.-J. Bi, J. Cosmol. Astropart. Phys. 3 (2015) 033.
[34] E. S. Seo and V. S. Ptuskin, Astrophys. J. **431**, 705 (1994).
[35] M. Ackermann *et al.*, Science **339**, 807 (2013).
[36] A. D. Panov *et al.*, Bull. Russ. Acad. Sci. Phys. **71**, 494 (2007).
[37] H. S. Ahn *et al.*, Astrophys. J. Lett. **714**, L89 (2010).
[38] O. Adriani *et al.*, Science **332**, 69 (2011).
[39] M. Aguilar *et al.*, Phys. Rev. Lett. **114**, 171103 (2015).
[40] M. Aguilar *et al.*, Phys. Rev. Lett. **115**, 211101 (2015).
[41] J. R. Jokipii, Astrophys. J. **208**, 900 (1976).
[42] J. J. Engelmann, P. Ferrando, A. Soutoul, P. Goret, and E. Juliusson, Astron. Astrophys. **233**, 96 (1990).
[43] I. V. Moskalenko, A. W. Strong, J. F. Ormes, and M. S. Potgieter, Astrophys. J. **565**, 280 (2002).
[44] V. S. Ptuskin, I. V. Moskalenko, F. C. Jones, A. W. Strong, and V. N. Zirakashvili, Astrophys. J. **642**, 902 (2006).
[45] N. Tomassetti, Astrophys. J. Lett. **752**, L13 (2012).
[46] Y.-Q. Guo, Z. Tian, and C. Jin, Astrophys. J. **819**, 54 (2016).
[47] M. D'Angelo, P. Blasi, and E. Amato, Phys. Rev. D **94**, 083003 (2016).
[48] http://galprop.stanford.edu/.
[49] R. M. Neal, *Probabilistic Inference Using Markov Chain Monte Carlo Methods* (University of Toronto, Toronto, 1993).
[50] D. Gamerman, *Markov Chain Monte Carlo: Stochastic Simulation for Bayesian Inference* (Chapman and Hall, London, 1997).
[51] M. Aguilar *et al.*, Phys. Rev. Lett. **117**, 231102 (2016).
[52] http://www.srl.caltech.edu/ACE/ASC/level2/lvl2DATA_CRIS.html.
[53] J. J. Connell, Astrophys. J. Lett. **501**, L59 (1998).
[54] A. Lukasiak, in *International Cosmic Ray Conference* (1999), Vol. 3, p. 41.
[55] J. A. Simpson and M. Garcia-Munoz, Space Sci. Rev. **46**, 205 (1988).
[56] T. Hams *et al.*, Astrophys. J. **611**, 892 (2004).
[57] O. Adriani *et al.*, Astrophys. J. **765**, 91 (2013).
[58] L. J. Gleeson and W. I. Axford, Astrophys. J. **154**, 1011 (1968).
[59] https://solarscience.msfc.nasa.gov/SunspotCycle.shtml.
[60] D. H. Hathaway, R. M. Wilson, and E. J. Reichmann, J. Geophys. Res. **104**, 22375 (1999).
[61] J. S. George *et al.*, Astrophys. J. **698**, 1666 (2009).
[62] S.-J. Lin, Q. Yuan, and X.-J. Bi, Phys. Rev. D **91**, 063508 (2015).
[63] G. Di Bernardo, C. Evoli, D. Gaggero, D. Grasso, and L. Maccione, J. Cosmol. Astropart. Phys. 3 (2013) 036.
[64] A. Kolmogorov, Akad. Nauk SSSR Doklady **30**, 301 (1941).
[65] R. H. Kraichnan, Phys. Fluids **8**, 1385 (1965).
[66] M. Aguilar *et al.*, Phys. Rev. Lett. **113**, 121102 (2014).
[67] C. S. Shen, Astrophys. J. Lett. **162**, L181 (1970).
[68] A. K. Harding and R. Ramaty, *International Cosmic Ray Conference* 2, 92 (1987).
[69] L. Zhang and K. S. Cheng, Astron. Astrophys. **368**, 1063 (2001).
[70] O. Adriani *et al.*, Phys. Rev. Lett. **105**, 121101 (2010).
[71] M. Aguilar *et al.*, Phys. Rev. Lett. **117**, 091103 (2016).
[72] X.-J. Huang, C.-C. Wei, Y.-L. Wu, W.-H. Zhang, and Y.-F. Zhou, Phys. Rev. D **95**, 063021 (2017).
[73] T. Li, arXiv:1612.09501.
[74] J. Feng and H.-H. Zhang, arXiv:1701.02263.
[75] I. Cholis, D. Hooper, and T. Linden, arXiv:1701.04406.
[76] AMS-02 Collaboration, in AMS Five Years Data Release, http://www.ams02.org/, 2016.
[77] T. Kamae, N. Karlsson, T. Mizuno, T. Abe, and T. Koi, Astrophys. J. **647**, 692 (2006).
[78] T. Delahaye, R. Lineros, F. Donato, N. Fornengo, J. Lavalle, P. Salati, and R. Taillet, Astron. Astrophys. **501**, 821 (2009).
[79] M. Pohl and J. A. Esposito, Astrophys. J. **507**, 327 (1998).
[80] J. M. Clem, D. P. Clements, J. Esposito, P. Evenson, D. Huber, J. L'Heureux, P. Meyer, and C. Constantin, Astrophys. J. **464**, 507 (1996).
[81] S. D. Torre *et al.*, Adv. Space Res. **49**, 1587 (2012).
[82] L. Maccione, Phys. Rev. Lett. **110**, 081101 (2013).
[83] M. S. Potgieter, E. E. Vos, M. Boezio, N. De Simone, V. Di Felice, and V. Formato, Sol. Phys. **289**, 391 (2014).
[84] R. Kappl, Comput. Phys. Commun. **207**, 386 (2016).
[85] E. C. Stone, A. C. Cummings, F. B. McDonald, B. C. Heikkila, N. Lal, and W. R. Webber, Science **341**, 150 (2013).
[86] A. C. Cummings, E. C. Stone, B. C. Heikkila, N. Lal, W. R. Webber, G. Jóhannesson, I. V. Moskalenko, E. Orlando, and T. A. Porter, Astrophys. J. **831**, 18 (2016).
[87] I. V. Moskalenko, A. W. Strong, S. G. Mashnik, and J. F. Ormes, Astrophys. J. **586**, 1050 (2003).
[88] D. Hooper, T. Linden, and P. Mertsch, J. Cosmol. Astropart. Phys. 3 (2015) 021.
[89] M.-Y. Cui, Q. Yuan, Y.-L. Sming Tsai, and Y.-Z. Fan, arXiv:1610.03840.
[90] A. Cuoco, M. Kramer, and M. Korsmeier, arXiv:1610.03071.
[91] F. Donato, D. Maurin, P. Salati, A. Barrau, G. Boudoul, and R. Taillet, Astrophys. J. **563**, 172 (2001).
[92] G. Giesen, M. Boudaud, Y. Génolini, V. Poulin, M. Cirelli, P. Salati, and P. D. Serpico, J. Cosmol. Astropart. Phys. 9 (2015) 023.
[93] S.-J. Lin, X.-J. Bi, J. Feng, P.-F. Yin, and Z.-H. Yu, arXiv:1612.04001.